Electro-Optic Effect of Nonchiral Smectic C Liquid Crystal Mode with Negative Dielectric Anisotropy

Chang-Jae Yu, Eunje Jang, and Sin-Doo Lee
School of Electrical Engineering #32, Seoul National University, Kwanak P.O. Box 34, Seoul 151-742, Korea

Abstract

We report on an analog electro-optic effect in a nonchiral smectic C (NSC) liquid crystal (LC) mode with negative dielectric anisotropy in a transverse electrode configuration. Two-dimensional numerical simulations are executed to evaluate the display performances. The analog gray scales in the NSC LC mode are obtained in a dielectrically driving scheme.

1. Introduction

A variety of liquid crystal display (LCD) modes [1-5] have been reported to improve the performance such as wide viewing and fast response properties. In the approaches [1,2] based on nematic liquid crystals (NLCs), additional complex processes for alignment are often involved. For various display configurations [3-4] using ferroelectric liquid crystals (FLCs) with spontaneous polarization, it is difficult to obtain the uniform alignment in large area since the polar nature of delicate interfacial interactions between treated substrates and the FLC molecules produces zigzag defacts [3] and/or stripe domains.

Recently, an electro-optic (EO) effect of a nonchiral smectic C (NSC) LC in a twisted geometry [6] has been theoretically predicted and the EO properties of the NSC LC layer in a transverse electrode structure [7] has been experimentally studied to explore the probability of practical applications. Unlike FLC materials, In the NSC LC modes, analog optical modulation was achieved by means of the dielectric anisotropy ($\Delta\varepsilon$).

In this work, we demonstrated experimentally a fast analog EO effect of NSC LC with negative dielectric anisotropy in a transverse electrode configuration and analyzed the display performances using numerical simulations based on a relaxation method [8] together with the 2x2 Jones matrix method [9]. The NSC LC mode exhibits wide and symmetric viewing properties with no additional compensation films. Moreover, using a dielectrically driving scheme as employed in the NLC mode, analog gray scales are naturally obtained.

2. Operation Principle

Figure 1 shows the operation principle of our NSC LC mode with negative dielectric anisotropy $\Delta\varepsilon$. Consider a sample cell of an NSC LC with $\Delta\varepsilon<0$, in which the NSC LC molecules are aligned antiparallel to glass substrates. The interdigital electrodes are patterned on

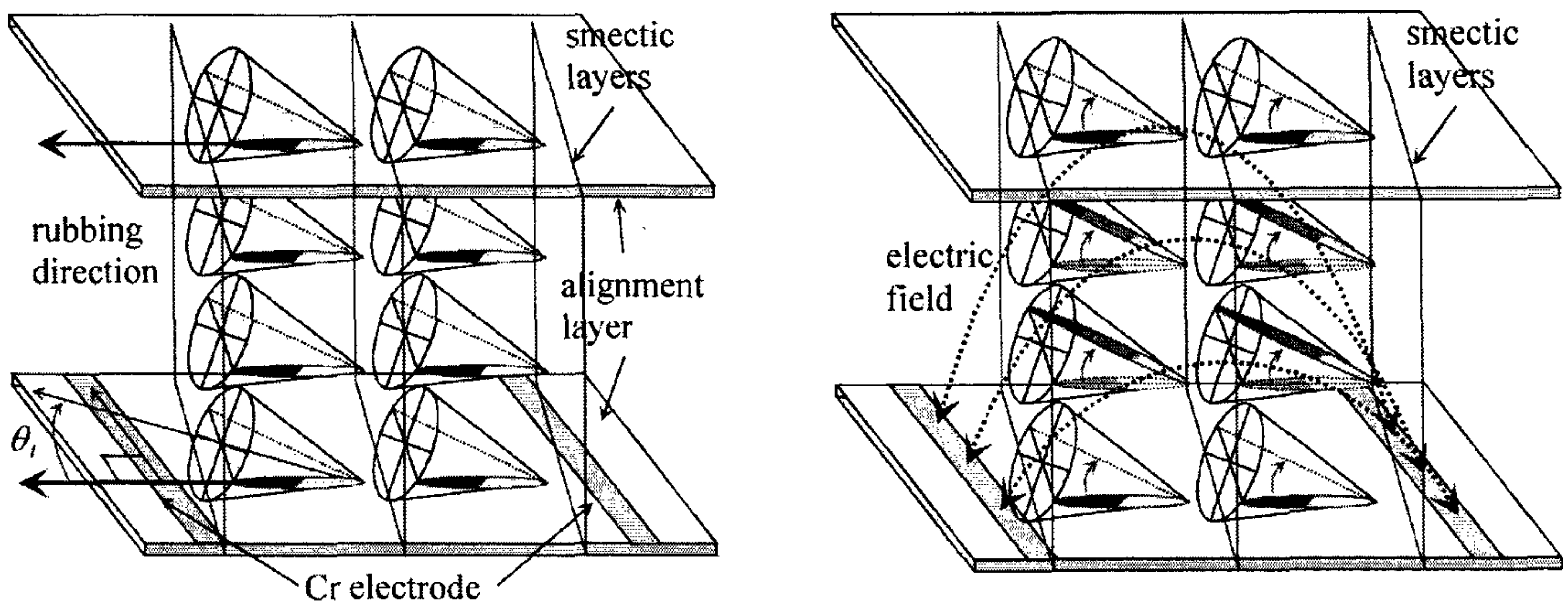

(a) (b)

Figure 1. The operation principle of the NSC LC mode with negative dielectric anisotropy: (a) The absence of an external electric field (dark state) and (b) the presence of an electric field (bright state).

only one of the substrates. The smectic layers make an angle of the molecular tilt in the NSC phase with respect to the transverse electrodes and the rubbing directions are perpendicular to the electrodes on the substrate.

As shown in Fig. 1 (a), in the absence of an electric field (dark state), the director of the NSC LC molecules aligns along the rubbing direction and is optically similar to that of a planar NLC. Except for the tilt of smectic layers, this structure of the NSC LC in the transverse electrode configuration corresponds exactly to a homogeneously aligned NLC structure. Therefore, a linearly polarized light, which is incident along the rubbing direction on one of the glass substrates, is blocked completely by the crossed analyzer.

On the other hand, when an electric field is presented (bright state), the NSC LC molecules rotate on the induced smectic C cone since the cone structure is energetically favored. The director of the NSC LC molecules with $\Delta\varepsilon<0$ tends to rotate perpendicular to the applied electric field as shown in Fig. 1(b). With increasing the applied electric field, the director finally reaches 180° of the azimuthal angle. In this situation, when a linearly polarized light is incident parallel to the rubbing direction, a phase modulation is achieved and thus optical transmission is produced.

3. Numerical Model

In a simple director model with one-dimensional (1-D) deformation where the LC director varies only in one direction and is independent of the others, the director configuration and the optical transmission cannot be calculated in the cell structure with the patterned electrodes that generate nonuniform electric fields. In our transverse electrode configuration, the variation of the NSC LC director along the direction of electrodes, denoted by y-axis, is ignored only. In the coordinate system, the direction of the applied electric field and the normal direction to the substrates are denoted by the x and z-axes, respectively.

Since the variations of the azimuthal angle of the director and the electric potential along the y-direction are negligible, both the director configuration and the potential distribution can be calculated in 2-D. Using a relaxation method [8] based on the dynamic equation of the director and the discrete version of the equation [10], the equilibrium director profiles can be calculated.

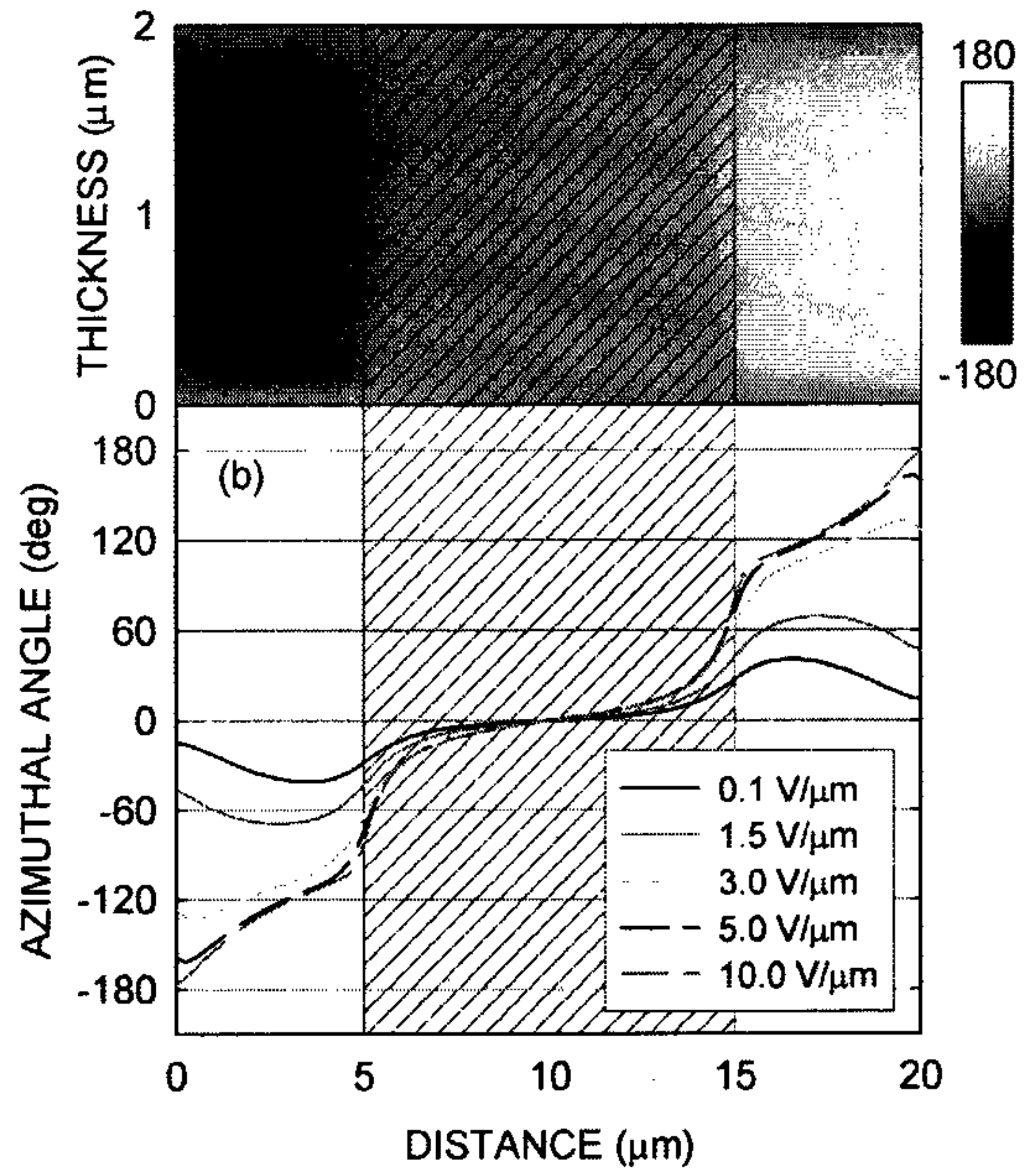

Figure 2. Numerical simulations for the azimuthal angle of the NSC LC director: (a) the 2-D gray scale map for the azimuthal angle of the NSC LC director at 5.0 V/μm. (b) the profiles of the azimuthal angle at various applied electric field in the mid-layer. The hatched region depicts the electrode.

Figure 2 shows numerical simulations for the azimuthal angle of the director. The distance across the transverse electrode is denoted by the horizontal axis. In Fig. 2(a), the azimuthal angle of the director at 5.0 V/μm is represented by 2-D gray scale map and the vertical axis depicts the cell thickness. As shown in Fig. 2(b), the configuration of the azimuthal angle in one side of the electrode is asymmetric with respect to the other side of the electrode, represented as a hatched region, at a given electric potential. Figure 2 (b) shows the configuration of the azimuthal angle at the mid-layer (thickness = 1 μm) at various applied voltages. With increasing the applied voltage, the azimuthal angle reaches ±180°. It should be noted that two states, ±180° of the azimuthal angles, are equivalent.

One interesting point is that the azimuthal angle of the director at half region between two transverse electrodes is favored at 0° for the low fields and at 180° for the high fields.

Using the profiles of the azimuthal angle obtained in Fig. 2, the optical transmittance averaged over an active region except for the region of the Cr electrode

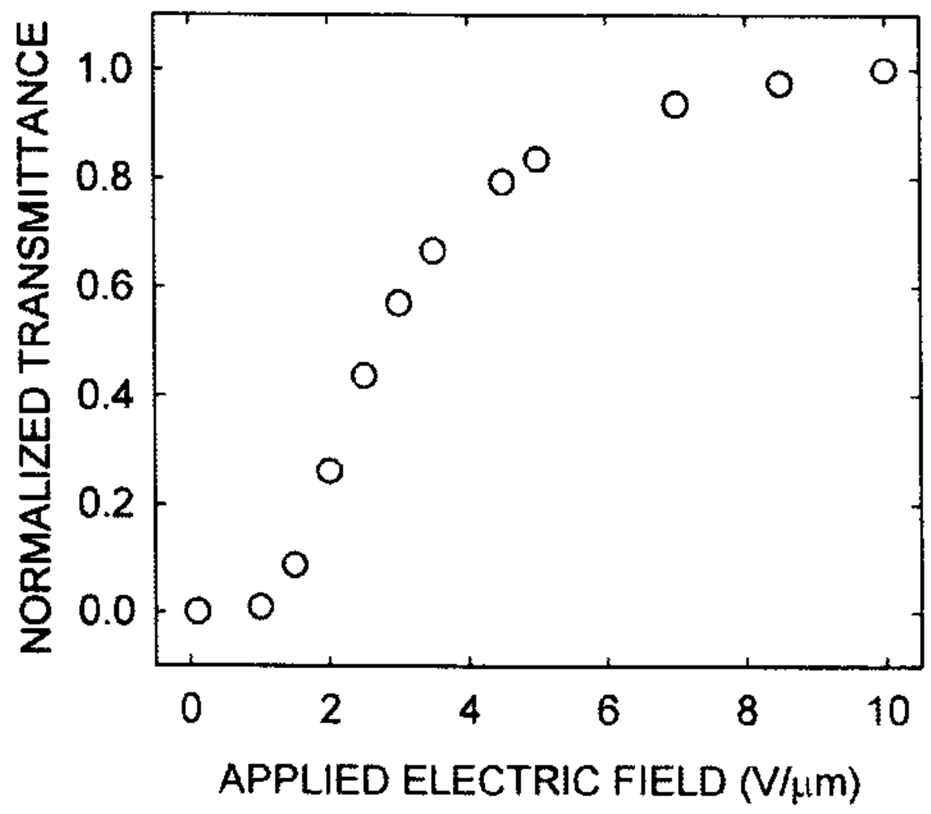

Figure 3. Numerical simulations of NSC LC mode for the average EO transmittance over active region under crossed polarizers.

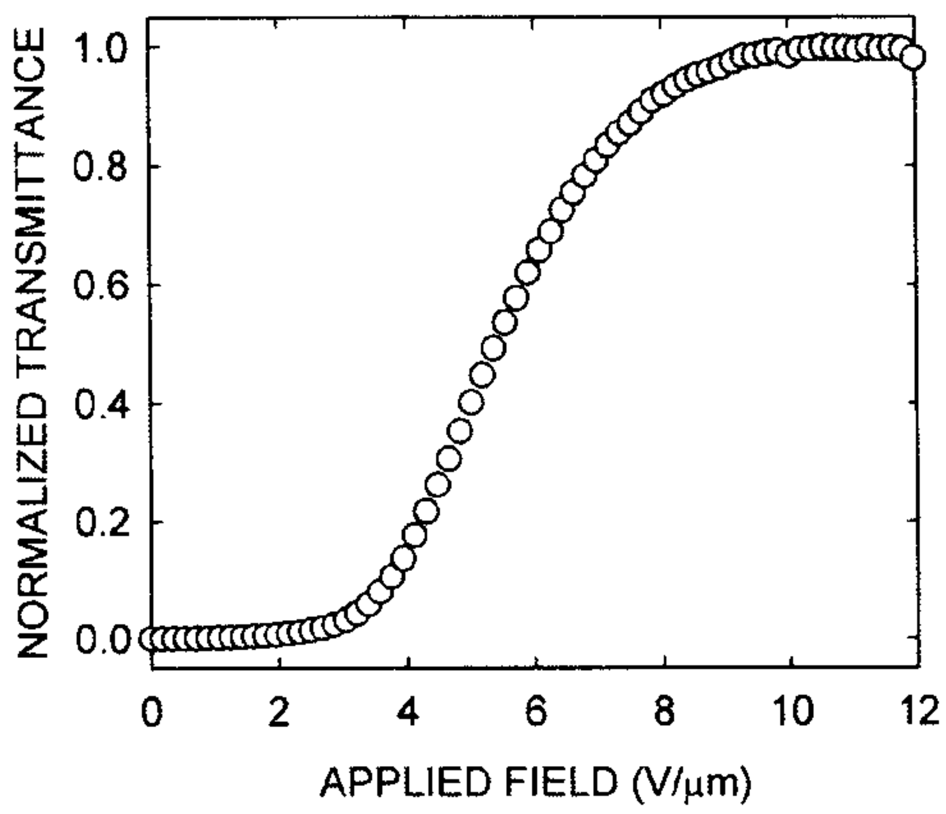

Figure 4. The EO transmittance through the NSC LC cell of IS-5511 under crossed polarizers.

is obtained using the 2x2 Jones matrix method [9]. The calculated transmittance was shown in Fig. 3 as a function of the applied voltage. As shown in Fig. 3, the EO transmittance increases monotonically with increasing the applied voltage above a certain threshold [11].

4. Experimental Results and Discussion

The transverse electrode configuration was designed using glass substrates, on one of which interdigital electrodes were prepared. The parallel electrodes were made by etching the Cr layer in an oppositely overlapped comb pattern. The separation between two electrodes was about 10 μm. The alignment layer of AL3046 (Japan Synthetic Rubber Co., Japan) was coated on the inner surface of the substrates and rubbed unidirectionally to produce homogeneous alignment. The cell was assembled such that the rubbing direction on the one surface was parallel to one of the crossed polarizers. Note that the rubbing directions on the two substrates were antiparallel to each other.

The NSC LC material used in this work was IS-5511 with negative dielectric anisotropy ($\Delta\varepsilon$ = -0.21) of Merck Co. Ltd. The tilt angle of IS-5511 in the smectic C phase is about 22.5° with respect to the normal direction to the smectic layers.

In Fig. 4, continuous gray scales of the NSC LC cell were shown as a function of the applied electric field of a bipolar square waveform at 30 Hz. With increasing the applied field above a certain threshold [11] of 2.3 V/μm, the EO transmittance increases monotonically as expected from the numerical simulations in Fig. 3.

The dynamic EO response of the NSC LC cell was measured using the applied field at 50 Hz as shown in Fig. 5. It should be noted that the NSC LC cell can be operated with a bipolar square waveform by means of the dielectric anisotropy like the NLC case. In the dielectrically driving scheme, the measured rising and falling times were 3.2 and 5.6 ms, respectively.

Figure 6 shows the iso-contrast map of the NSC LC cell with no compensation film. The vertical axis (*y*-axis) represents the direction of the transverse electrodes. Since the horizontal axis (*x*-axis) is parallel to the direction of the applied electric field, the NSC LC molecules with negative dielectric anisotropy reorient away from the rubbing direction.

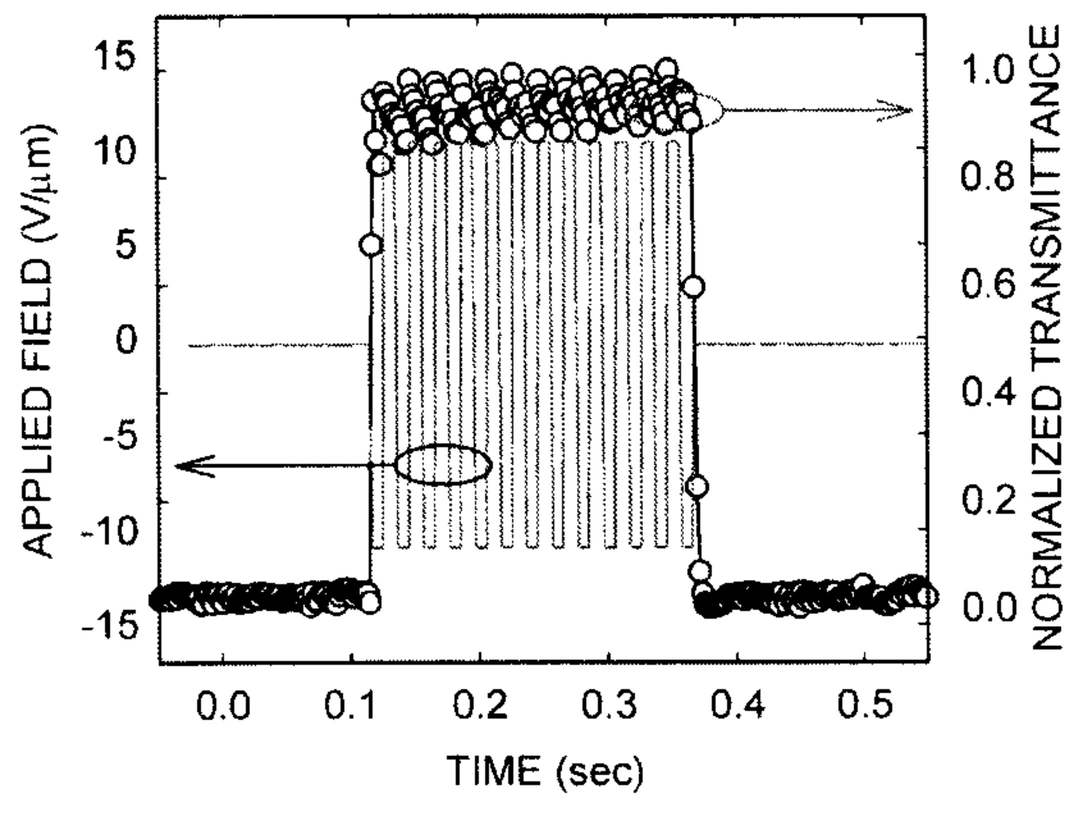

Figure 5. The dynamic EO response of the NSC LC cell to the applied field at 50 Hz.

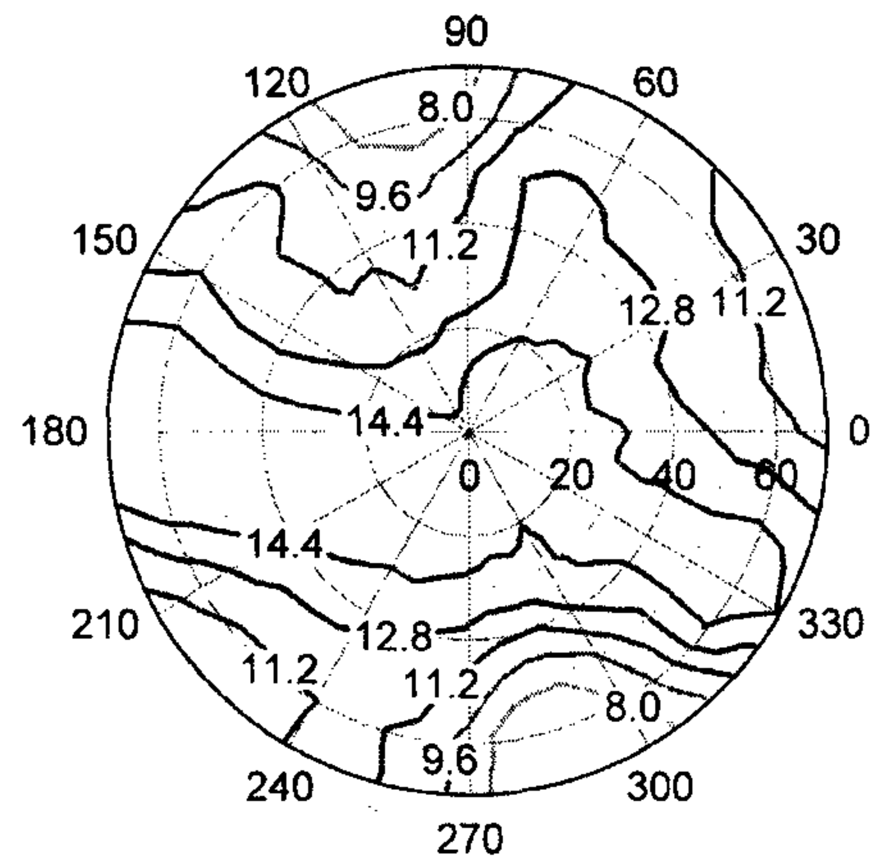

Figure 6. The iso-contrast map in the NSC LC cell for IS-5511 (not calibrated).

No contrast inversion is seen in the range of the viewing angle (up to 70°) we measured.

5. Conclusion

We demonstrated theoretically and experimentally a fast analog EO effect of the NSC LC mode with negative dielectric anisotropy in a transverse electrode configuration. The analog gray scales were obtained in the dielectrically driving scheme as in the NLC mode. The rising and falling times were found to be 3.2 and 5.6 ms, respectively. Further studies such as the effect of bending smectic layers near electrodes remain to be carried out.

6. Acknowledgements

This work was supported in part by Ministry of Information and Communication through Advanced Backbone IT technology development project. The authors are grateful to M.-O. Jin of Merck Ltd. Co., Korea for measuring iso-contrast maps.

7. References

[1] M. Oh-e, M. Ohta, S. Aratani, and K. Kondo, Proc. IDRC '95, p.577 (1995).

[2] M. Schadt, H. Seiberle, and A. Schuster, Nature (London) 381, 212 (1996).

[3] N. A. Clark and S. T. Lagerwall, Appl. Phys. Lett. 36, 899 (1980).

[4] L. A. Beresnev, L. M. Blinov, D. I. Dergachev, and S. B. Kondratev, JETP Lett. 46, 413 (1987).

[5] J.-H. Lee, C.-J. Yu, D.-H. You, and S.-D. Lee, Proc. IDW '99, p.129 (1999).

[6] S.-W. Suh, S.-D. Lee, and J. S. Patel, J. Korean Phys. Soc. 29, 399 (1996).

[7] C.-J. Yu, J.-Y. Kim, and S.-D. Lee, Appl. Phys. Lett. 80, 1111 (2002).

[8] See, for example, W. H. Press, B. P. Flannery, S. A. Teukolsky, and W. T. Vetterling, Numerical Recipes: The Art of Scientific Computing, Cambridge University Press, Cambridge (1986).

[9] P. Yeh, Optical Waves in Layered Media, John Wiley & Sons, Chichester (1988).

[10] H. Mori, E. C. Gartland, Jr., J. R. Kelly, and P. J. Bos, Jpn. J. Appl. Phys. 38, 135 (1999).

[11] P. G. de Gennes and J. Prost, The Physics of Liquid Crystals, Oxford University Press, New York (1993).